NOTES AND CORRESPONDENCE

The IMPROVE-1 Storm of 1–2 February 2001. Part IV: Precipitation Enhancement across the Melting Layer

CHRISTOPHER P. WOODS, JOHN D. LOCATELLI, AND MARK T. STOELINGA

Department of Atmospheric Sciences, University of Washington, Seattle, Washington

(Manuscript received 18 July 2006, in final form 3 April 2007)

ABSTRACT

Previous model simulations indicate that in stratiform precipitation, the precipitation rate can increase by 7% in the melting layer through direct condensation onto melting snow and the resultant cooled rain. In the present study, a model simulation of stratiform precipitation in a wide cold frontal rainband indicates that the precipitation rate can also increase by 5% in the melting layer through accretion, by melting snow and rain, of additional cloud water produced by the latent cooling of the ambient air associated with melting snow. The contribution of the combined processes, and therefore the additional precipitation gained through the latent cooling of melting snow within the melting layer, may contribute as much as 10% to the precipitation rate in stratiform precipitation.

1. Introduction

Numerous studies have focused on microphysics near and within the melting layer (e.g., Oraltay and Hallett 2005; Stewart et al. 1984; Drummond et al. 1996) and modeling of such regions (e.g., Szyrmer and Zawadzki 1999). In these studies, the behavior of melting snowflakes has been intensively studied and has been shown to play a role in the processes related to precipitation development. Lifting may lead to cloud liquid water formation (and collection by melting snow and rain) in the melting layer. This lifting may result from mesoscale circulations caused by uneven melting rates, frontal lifting, or frontal lifting enhanced by proximity to the rain/snow boundary. See, for example, Lin and Stewart (1986), Szeto et al. (1988a,b), Houze (1993), and Szeto and Stewart (1997).

Stewart (1992) discussed the potential for melting particles to grow by condensation given a large temperature gradient between the melting particle and the environment. Szyrmer and Zawadzki (1999) modeled this process and found that the increase in precipitation depended on the saturation of the air. If the air remained unsaturated during this process, the mass added to the melting snow through condensation came from the evaporation of small raindrops resulting in no net increase in precipitation. If the air was saturated, this process resulted in an increase in precipitation. However, the increase of the mass of a melting snow particle was less than 7% of the original mass of the particle.

Another potential source of mass leading to an increase in precipitation in the melting layer is the accretion, by melting snow and rain, of cloud water resulting from additional condensation due to the cooling of the layer associated with melting of frozen precipitation particles. This possibility has been discussed by Rutledge and Hobbs (1983), Stewart et al. (1984), and Szeto and Stewart (1997). However, the additional precipitation due to this mechanism has never been quantified.

The extensively modeled and studied storm of 1–2 February 2001 (Evans et al. 2005; Locatelli et al. 2005; Woods et al. 2007) during the Improvement of Microphysical Parameterization through Observational Verification Experiment (IMPROVE; Stoelinga et al. 2003) presents an opportunity to quantify the additional pre-

Corresponding author address: Mark T. Stoelinga, Department of Atmospheric Sciences, University of Washington, Box 351640, Seattle, WA 98195.
E-mail: stoeling@atmos.washington.edu

DOI: 10.1175/2007JAS2247.1

cipitation production provided by the cooling in the melting layer discussed in the preceding paragraph.

2. Model description

The mesoscale model utilized in this paper is version 3.7.0 of the fifth-generation Pennsylvania State University (PSU)–National Center for Atmospheric Research (NCAR) Mesoscale Model (MM5; Grell et al. 1994) and is identical to that used in Woods et al. (2007). This is similar to the Locatelli et al. (2005) model run of the 1–2 February storm in terms of time period, domain configuration, and physics options, with the following two exceptions. The Woods et al. model run used the NCAR–NCEP reanalysis gridded data as a first guess, which produced a superior simulation of the storm's wide cold frontal rainband (WCFR). Also, Woods et al. used the Reisner–Thompson microphysical scheme as described by Thompson et al. (2004) with the following modification. The Reisner–Thompson scheme utilizes the velocity–diameter relationship for cold-type snow particles from Locatelli and Hobbs (1974) and, since cold-type particles most closely matched those observed in the upper levels of this WCFR by Evans et al. (2005), the mass–diameter relationship in the Reisner–Thompson scheme was changed to also correspond to the observed cold-type relationship reported in Locatelli and Hobbs (instead of the relationship for constant-density spheres). Complete discussion of this modification and its improved depiction of the WCFR is given in Woods et al. (2007).

3. Precipitation formation and growth in the WCFR

a. Major mechanisms of precipitation growth

Evans et al. (2005) provide a complete description of precipitation growth at different levels of the precipitating cloud mass for the 1–2 February 2001 event, as determined from observations including those of the University of Washington's Convair-580 aircraft. Using particle imagery to determine particle size distributions and habit types and employing mass– and velocity–diameter relationships for the observed habit types, they estimated the precipitation rate at each level that the aircraft flew. They also estimated precipitation growth based on the vertical gradient of precipitation rate (assuming a steady-state environment) and inferred the dominant mechanisms of growth based on the presence (or absence) of various hydrometeor species.

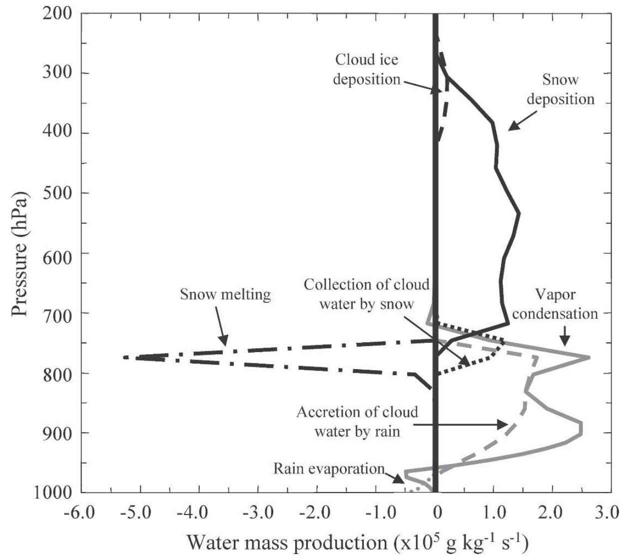

FIG. 1. Vertical profile of primary water mass production terms (labeled) in the 1–2 Feb 2001 WCFR valid at 0100 UTC 2 February 2001. The profile is taken at approximately the midpoint of the WCFR.

Their analyses indicated that precipitation growth was by deposition aloft (above the melting layer) and by riming of snow just above the melting layer and accretion of liquid water by melting snow and rain within the melting layer. The presence of cloud water near the melting level was attributed to enhanced lifting from a warm front, which was present at this level within the warm-type occluded frontal structure. Figure 1 shows a vertical profile from the model simulation, valid at 0100 UTC 2 February 2001, of the significantly active microphysical production terms within the middle of the WCFR simulation. Similar to what Evans et al. (2005) found in the observed case, the primary production terms for snow are vapor deposition throughout a deep layer above the melting level and the collection of cloud water by snow within and just above the melting level. Below the melting level, condensational production of cloud water, and subsequent collection by rain, resulted in additional precipitation growth.

Figure 2 shows a favorable comparison between the vertical profile of precipitation rate derived from the Convair-580 and that extracted from within the simulated WCFR. The strongest precipitation increase in the snow field occurred between 6.5 and 4.5 km. Another region of strong precipitation growth occurred between the melting layer and the ground. Both of these regions also correspond to regions of enhanced precipitation increases in the model simulation. The melting level is ~500 m higher in the model simulation

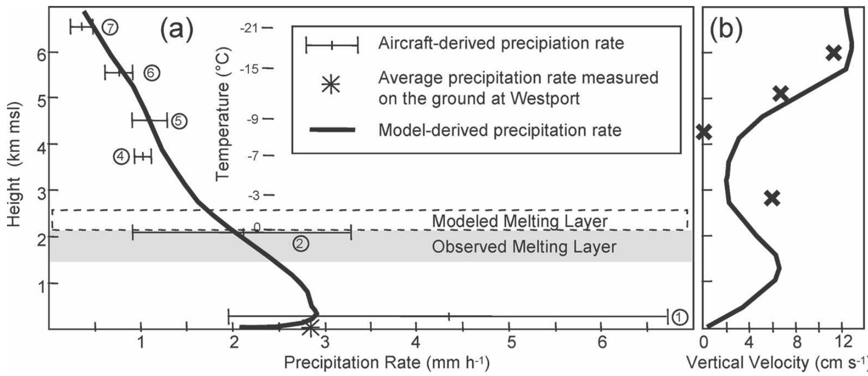

FIG. 2. (a) Adapted from Evans et al. (2005) showing aircraft-derived precipitation rate estimates from the Convair-580 horizontal flight legs in the 1–2 Feb 2001 WCFR. Model-derived precipitation rate (mm h^{-1}) corresponding to the location in the band where the Convair-580 flew is shown by the thick solid line. The gray-shaded and dotted boxes indicate the observed and modeled melting layers, respectively. The temperature scale corresponds to observed temperatures at the indicated heights. (b) Model-simulated vertical velocity (solid line, cm s^{-1}) in the 1–2 Feb 2001 WCRF. The bold "×" markers indicate vertical velocity estimates from the University of Washington (UW) Convair-580 aircraft described in Evans et al. (2005). Model results are valid at 0100 UTC 2 Feb 2001.

than in the observations. Tests with different initial conditions produced melting levels of different heights, some of which were closer to the observed, suggesting that the inaccuracy in melting layer height is largely due to limits on predictability of the synoptic-scale structure. We retained the present simulation as our "control" to maintain continuity with the control simulation used in Woods et al. (2007).

From the precipitation growth rate, Evans et al. estimated the vertical velocity by assuming maintenance of ice saturation and calculating the vertical velocity required to supply excess vapor at a rate equal to the observed precipitation growth rate. Their estimates of vertical velocity are shown with "×"s in Fig. 2b. These are in fairly good agreement with the vertical profile of vertical velocity extracted from the model simulation. The model simulation has enhanced regions of upward motion of 12–14 cm s^{-1} above 5 km, associated with the upper cold front, and a lesser maximum just above 1 km, associated with the warm frontal lifting. Although the maximum in upward motion above 5 km was larger in magnitude than that lower down (Fig. 2b), the lower region of upward motion produced more condensate and precipitation than that above 5 km, due to a larger rate of excess vapor supply at warm temperatures than at cold temperatures for the same vertical motion (cf. "accretion of cloud water by rain" at low levels to "snow deposition" at upper levels in Fig. 1).

Examination of the microphysical production terms in the model simulation indicates that ~75% of the total growth of precipitation reaching the ground in the WCFR occurred above the melting layer, primarily through vapor deposition, and ~20% resulted from the collection of cloud water (predominantly by rain, also by snow) produced by warm frontal lifting near the melting level. The remaining ~5% resulted from enhanced cloud water production and collection in the melting layer.

Figure 3 shows the model-simulated vertical gradient

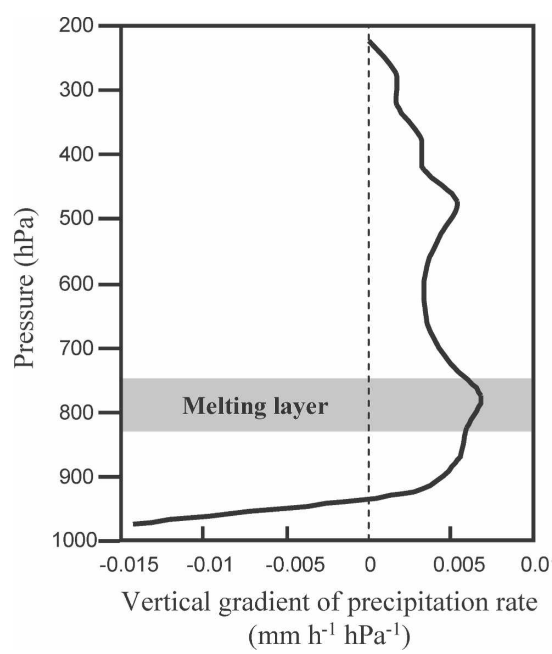

FIG. 3. Model-simulated downward vertical gradient of precipitation rate (given in Fig. 2) in the 1–2 Feb 2001 WCRF valid at 0100 UTC 2 Feb 2001.

of precipitation rate derived from the precipitation rate shown in Fig. 2. The maximum increase in precipitation rate occurs within the melting layer at ~775 hPa. This corresponds to the location of the maximum in vapor condensation and the combined collection of cloud water by snow and rain (Fig. 1). This leads us to believe that the latent cooling by the melting snow could be a factor in the increased collection of cloud water in this region.

b. *Precipitation enhancement across the melting layer*

To examine whether latent cooling by the melting snow was producing the maximum in vapor condensation in the melting layer, we performed an additional model simulation except with latent cooling due to melting snow withheld for 1 h prior to the time of the model results shown in Figs. 1–3. The melting of snow includes the processes in the model where snow is converted to rain by melting and snow is converted to rain through rain/snow collisions. The resulting cloud water field shows that the region of locally high cloud-water values previously existing immediately beneath the 0°C level (Fig. 4a) is absent in the no-cooling simulation (Fig. 4b). This lack of cloud water and associated lack of additional collection by falling precipitation diminished the precipitation rate by up to 5% in the no-cooling simulation.

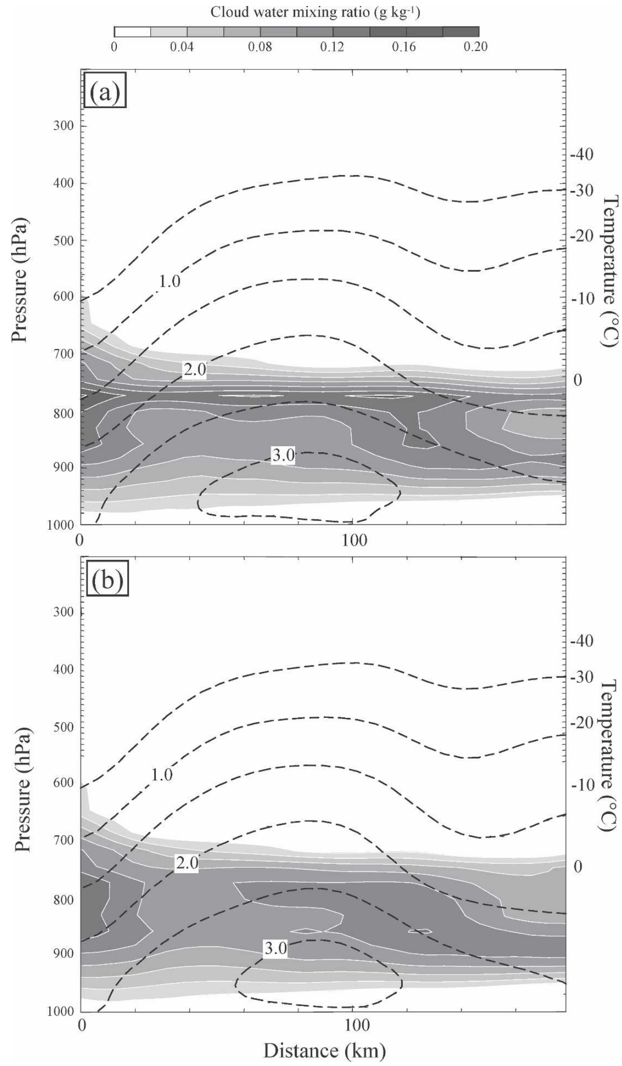

FIG. 4. (a) Vertical cross section through the WCFR for the model simulation valid at 0100 UTC 2 Feb 2001. Cloud liquid water mixing ratio is shown by the shaded contours (g kg^{-1}), and precipitation rate by the dashed contours every 0.5 mm h^{-1}. Temperatures are indicated every 10°C. (b) As in (a) except with the latent cooling effects of rain and snow collisions and melting snow turned off 1 h prior to the time of the cross section.

4. Discussion and conclusions

Although the mechanism described above (production and accretion of cloud liquid water through the diabatic effects of melting snow) is active in the present model and makes physical sense, the extent to which it may have occurred in the melting layer of the observed WCFR cannot be confirmed from our available observations. It is only known that the Convair-580 did encounter enhanced cloud water values near the melting layer.

An important consideration is the lack of the possibility of condensation onto the melting snow or rain in the melting layer in the Reisner–Thompson microphysical scheme used in our model simulations, as it is assumed that the surface area available for condensation onto such particles is negligible compared to that of a typical population of cloud droplets. However, this difference in surface area may be offset by the larger temperature difference between the melting snow and the ambient air as compared to the temperature difference of the cloud droplets and the ambient air. This is supported by modeling work (such as that carried out by Szyrmer and Zawadzki 1999), discussed in the introduction, that indicates these omitted processes can be significant, or at least on the order of the mechanism described in this paper. A further complication is that the accretion of cloud liquid water by rain or melting snow is not modeled in the Szyrmer and Zawadzki model formulation. Szyrmer and Zawadzki justify this omission by the low amount of cloud liquid water generated in their simulation (<0.15 g kg^{-1}).

The two microphysical processes discussed above—namely, condensation to form cloud drops and subsequent accretion by precipitation, and condensation directly onto "cooled" precipitation particles—are not mutually exclusive since they are both competing from the same source of water vapor. However, the dominant process might depend on the amount of cloud liquid water present in the melting layer due to lifting in that layer. If very little cloud liquid water is present, then the additional cloud liquid water produced through latent cooling could produce a size distribution that was too small to be effectively collected by the cooled melting snow and resultant cooled rain. In this case, condensation directly on the cooled melting snow and resultant cooled rain could dominate. On the other hand, if sufficient liquid water were present, then any additional condensation due to cooling of the ambient air would be on larger cloud drops that could be effectively collected leading to the dominance of the collection process in the melting layer.

The model simulation of Szyrmer and Zawadzki (1999) indicated that the precipitation rate could be increased by 7% in the melting layer through condensation on the latent-cooled melting snow and the resultant cooled rain. Our model simulation of stratiform precipitation in a WCFR indicates that the precipitation rate could be increased by 5% in the melting layer through the accretion, by melting snow and rain, of the additional cloud water produced by the latent cooling of the ambient air. In any case, since the latent cooling is fixed by the melting of the snow, the contribution of the combined processes and therefore the additional precipitation gained through the latent cooling of the melting snow in the melting layer is probably limited to less than 10% of the precipitation rate in stratiform precipitation. A microphysical model that includes both of these processes is likely needed to accurately determine the importance of each process relative to the other in the same storm.

Finally, while our model simulation utilized a horizontal grid spacing (12 km) typical of current operational forecast models and is generally thought to be adequate for representing stratiform precipitation, there is a broad range of scales of motion that are unresolved in our simulation and are known or hypothesized to influence microphysical processes. These include the effect of small-scale turbulence on droplet collisions and spectral broadening (e.g., see review by Jonas 1996) or the effect of shear-induced turbulence on production of cloud water and enhancement of riming and aggregation (Houze and Medina 2005). Therefore, a thorough examination of microphysical processes within the melting layer would require simulations that include some combination of higher-resolution and parameterization refinements to represent such processes.

Acknowledgments. We thank all of the participating scientific investigators, staff, and students for their tireless efforts in IMPROVE, and NOAA and NCAR for providing important facilities and personnel. This research was supported by Grants ATM-9908446 and ATM-0242592 from the National Science Foundation.

REFERENCES

Drummond, F. J., R. R. Rogers, S. A. Cohn, W. L. Ecklund, D. A. Carter, and J. S. Wilson, 1996: A new look at the melting layer. *J. Atmos. Sci.,* **53,** 759–769.

Evans, A. G., J. D. Locatelli, M. T. Stoelinga, and P. V. Hobbs, 2005: The IMPROVE-1 storm of 1–2 February 2001. Part II: Cloud structures and the formation of precipitation. *J. Atmos. Sci.,* **62,** 3456–3473.

Grell, G. A., J. Dudhia, and D. R. Stauffer, 1994: A description of the fifth-generation Penn State/NCAR Mesoscale Model (MM5). NCAR Tech. Note TN-398+STR, 122 pp. [Available from UCAR Communications, P.O. Box 3000, Boulder, CO 80307.]

Houze, R. A., Jr., 1993: *Cloud Dynamics*. Academic Press, 570 pp.

——, and S. Medina, 2005: Turbulence as a mechanism for orographic precipitation enhancement. *J. Atmos. Sci.,* **62,** 3599–3623.

Jonas, P. R., 1996: Turbulence and cloud microphysics. *Atmos. Res.,* **40,** 283–306.

Lin, C., and R. E. Stewart, 1986: Mesoscale circulations initiated by melting snow. *J. Geophys. Res.,* **91,** 13 299–13 302.

Locatelli, J. D., and P. V. Hobbs, 1974: Fall speeds and masses of solid precipitation particles. *J. Geophys. Res.,* **79,** 2185–2197.

——, M. T. Stoelinga, M. F. Garvert, and P. V. Hobbs, 2005: The IMPROVE-1 storm of 1–2 February 2001. Part I: Development of a forward-tilted cold front and a warm occlusion. *J. Atmos. Sci.,* **62,** 3431–3455.

Oraltay, R. G., and J. Hallett, 2005: The melting layer: A laboratory investigation of ice particle melt and evaporation near 0°C. *J. Appl. Meteor.,* **44,** 206–220.

Rutledge, S. A., and P. V. Hobbs, 1983: The mesoscale and microscale structure and organization of clouds and precipitation in mid-latitude cyclones. Part VIII: A model for the "seeder–feeder" process in warm frontal rainbands. *J. Atmos. Sci.,* **40,** 1185–1206.

Stewart, R. E., 1992: Precipitation particles in the transition region of winter storms. *Bull. Amer. Meteor. Soc.,* **73,** 287–296.

——, J. D. Marwitz, J. C. Pace, and R. E. Carbone, 1984: Characteristics through the melting layer of stratiform clouds. *J. Atmos. Sci.,* **41,** 3227–3237.

Stoelinga, M. T., and Coauthors, 2003: Improvement of Microphysical Parameterization through Observational Verification Experiment. *Bull. Amer. Meteor. Soc.,* **84,** 1807–1826.

Szeto, K. K., and R. E. Stewart, 1997: Effects of melting on frontogenesis. *J. Atmos. Sci.,* **54,** 689–702.

——, C. A. Lin, and R. E. Stewart, 1988a: Mesoscale circulations forced by melting snow. Part I: Basic simulations and dynamics. *J. Atmos. Sci.,* **45,** 1629–1641.

——, R. E. Stewart, and C. A. Lin, 1988b: Mesoscale circulations forced by melting snow. Part II: Application to meteorological features. *J. Atmos. Sci.,* **45,** 1642–1650.

Szyrmer, W. S., and I. Zawadzki, 1999: Modeling of the melting layer. Part I: Dynamics and microphysics. *J. Atmos. Sci.,* **56,** 3573–3592.

Thompson, G., R. M. Rasmussen, and K. Manning, 2004: Explicit forecasts of winter precipitation using an improved bulk microphysics scheme. Part I: Description and sensitivity analysis. *Mon. Wea. Rev.,* **132,** 519–542.

Woods, C. P., M. T. Stoelinga, J. D. Locatelli, and P. V. Hobbs, 2007: The IMPROVE-1 storm of 1–2 February 2001. Part III: Sensitivity of a mesoscale model simulation to the representation of snow particle types and testing of a bulk microphysical scheme with snow habit prediction. *J. Atmos. Sci.,* **64,** 3927–3948.